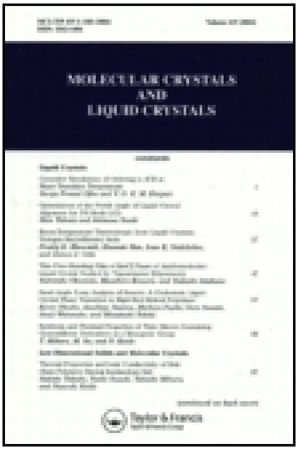

Molecular Crystals and Liquid Crystals
Publication details, including instructions for authors and subscription information:
http://www.tandfonline.com/loi/gmcl20

Asymmetric Aberration Pattern at Light-Beam Self-Action in NLC Doped with Stilbene Dye

A. S. Zolot'ko [a], I. A. Budagovsky [a], M. P. Smayev [a] & M. I. Barnik [b]

[a] P. N. Lebedev Physical Institute, Moscow, Russia
[b] A. V. Shubnikov Institute of Crystallography, Moscow, Russia

Version of record first published: 22 Sep 2010

To cite this article: A. S. Zolot'ko, I. A. Budagovsky, M. P. Smayev & M. I. Barnik (2008): Asymmetric Aberration Pattern at Light-Beam Self-Action in NLC Doped with Stilbene Dye, Molecular Crystals and Liquid Crystals, 488:1, 11-22

To link to this article: http://dx.doi.org/10.1080/15421400802240078

Mol. Cryst. Liq. Cryst., Vol. 488, pp. 11–22, 2008

ISSN: 1542-1406 print/1563-5287 online
DOI: 10.1080/15421400802240078

Asymmetric Aberration Pattern at Light-Beam Self-Action in NLC Doped with Stilbene Dye

A. S. Zolot'ko[1], I. A. Budagovsky[1], M. P. Smayev[1], and M. I. Barnik[2]
[1]P. N. Lebedev Physical Institute, Moscow, Russia
[2]A. V. Shubnikov Institute of Crystallography, Moscow, Russia

Light-beam interaction with nematic liquid crystals doped with stilbene dye DEANS (4-diethylamino-4′-nitrostilbene) has been studied experimentally. For the homeotropic sample, a conventional ring-shaped aberration self-focusing pattern (related to the dye-induced orientational nonlinearity) and the memory effect were observed. For the planar sample, a complex asymmetric aberration pattern qualitatively different from the concentric-ring system was observed for the first time. The study of the phenomenon allowed us to assume that this pattern is due to the bulk photorefractive effect.

Keywords: nematic liquid crystals; optical nonlinearity; photorefractive effect; self-phase modulation; stilbene dye

INTRODUCTION

It is well known that incorporation of small amounts of dyes into nematic liquid crystals (NLCs) can significantly increase the orientational optical nonlinearity and lead to new optical phenomena and applications [1–11]. Thus, for example, azodyes increase orientational nonlinearity of NLCs by two orders of magnitude and make it sign-variable [2–4]. Azodye-doped NLCs feature the memory effect [8], the director-field bistability [9], and the possibility of image storage, processing and recognition [10,11].

The authors are grateful to B. A. Umansky for helpful discussions and N. I. Lyukhanov for his help in performing experiments. The study was supported by the Russian Foundation for Basic Research (project no. 05-02-17418). I.A.B. and M.P.S. are grateful to the Program of the Russian Academy of Sciences “Support of Young Scientists”. M.P.S is also indebted to the Russian Science Support Foundation.

Address correspondence to A. S. Zolot'ko, P. N. Lebedev Physical Institute, Leninsky pr. 53, Moscow 119991, Russia. E-mail: zolotko@lebedev.ru

In our work we perform detailed experimental study of the light-beam interaction with NLCs doped with a stilbene dye. The dye DEANS used is similar in structure to azodye DEANAB, whose nonlinear-optical properties were studied previously in detail [4,12]. Some results on the nonlinear-optical properties of NLC with DEANS were briefly reported in [13,14].

EXPERIMENTAL

The studies were carried out on the homeotropically and planarly aligned cells of the liquid-crystalline material ZhKM-1277 doped with stilbene dye DEANS (4-diethylamino-4′-nitrostilbene, 0.1 and 0.025 wt %), as well as on the planarly aligned cell of ZhKM-13N doped with 0.1 wt % DEANS.

The structural formula of DEANS has the form

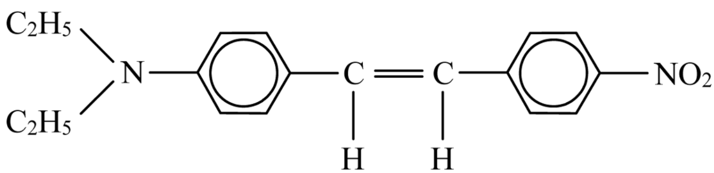

The liquid-crystalline material ZhKM-1277 (NIOPIK, Russia) is a mixture of biphenyls and esters. This mixture exhibits a nematic phase in the temperature range from -20°C to $+60^\circ$C and has a positive low-frequency dielectric anisotropy ($\Delta\varepsilon = 12.1$ at $f = 1$ kHz and $t = 20^\circ$C). The refractive indices of the extraordinary ($n_{||} = \sqrt{\varepsilon_{||}}$) and ordinary ($n_\perp = \sqrt{\varepsilon_\perp}$) waves are 1.71 and 1.52, respectively ($\lambda = 589$ nm). The liquid-crystalline material ZhKM-13N (NIOPIK, Russia) has a negative low-frequency dielectric anisotropy ($\Delta\varepsilon = -4.1$).

The cell thickness was $L = 100\,\mu$m. The planar alignment was produced by rubbing polyimide layers on the glass substrates with the electrodes from indium and tin oxides. Homeotropic alignment was obtained using chromium stearyl chloride.

The dye DEANS dissolved in ZhKM-1277 has an absorption band peaked at 460 nm. At $\lambda = 473$ nm the absorption coefficients of the extraordinary and ordinary waves are $\alpha_{||} = 410\,\text{cm}^{-1}$ and $\alpha_\perp = 90\,\text{cm}^{-1}$ (for dye concentration of 0.1 wt %).

Schematic representation of the experimental setup is shown in Figure 1. The light sources were argon and solid-state lasers emitting at 458, 473, 488, 515, and 532 nm. The linear-polarization direction could be changed with a double Fresnel rhomb (DFR). The light beam

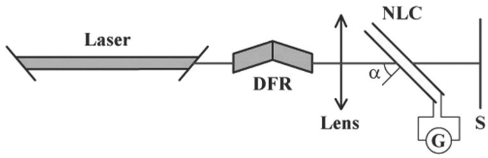

FIGURE 1 Schematic representation of the experimental setup: (DFR) double Fresnel rhomb, (G) voltage generator, and (S) screen.

was focused into the NLC cell by a lens (f = 16 or 18 cm); the transmitted radiation was observed on the screen S. The incidence angle α was changed by rotating the NLC cell about the vertical axis (the α values are taken as positive if the cell is rotated counterclockwise). The unperturbed NLC director was in the horizontal plane (the plane of the light-wave incidence). AC (3 kHz) or DC voltage could be applied to the cell. The polarity of the DC voltage was considered positive if the input (with respect to the light beam) NLC substrate was an anode. The experiments were carried out at room temperature.

RESULTS

Light Interaction with Homeotropically Aligned NLCs

A characteristic aberration pattern of self-focusing was observed in the cross-section of the beam ($\lambda = 473$–515 nm) transmitted through NLC samples. The times of its development and relaxation (~10 s) correspond to orientational processes [15]. The number of the aberration rings N in the steady-state pattern increases with the light beam power P (Fig. 2). At the normal incidence ($\alpha = 0°$), the dependence N(P) has a threshold. At sufficiently high P, the aberration ring number saturates. Application of AC electric field suppresses the pattern, which confirms the orientational origin of the nonlinearity.

The Freedericksz threshold for the dye-doped (0.1%) nematic host $P_{th} = 2.8$ mW ($\lambda = 488$ nm) is much less than $P_{th} = 110$ mW for the undoped ZhKM-1277. For the cell with lower dye concentration (0.025%), the threshold was about four times higher. For $\lambda = 515$ and 473 nm, the dependences N(P) were similar to those for $\lambda = 488$ nm. The Freedericksz threshold weakly depends on the light wavelength.

For the ordinarily polarized light obliquely incident at angles close to zero, we observed oscillations of the ring number resulting from the energy exchange between the normal waves inside the NLC cell [16,17]. The presence of these oscillations additionally confirms the orientational origin of the nonlinearity.

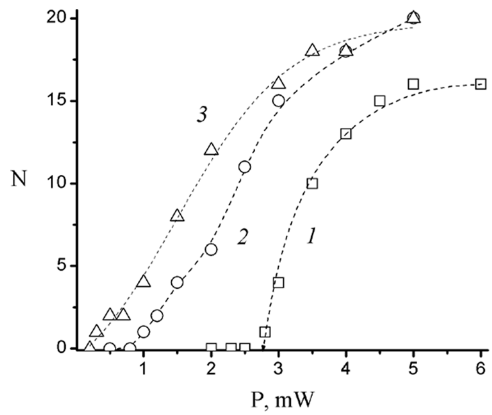

FIGURE 2 The dependences of the aberration ring number N (self-focusing) in the cross-section of the beam ($\lambda = 488\,\text{nm}$) passed through the homeotropic NLC ZhKM-1277 + 0.1% DEANS on the beam power P at various angles of incidence: $\alpha =$ (*1*) 0°, (*2*) 10°, (*3*) 30°.

The nonlinearity enhancement factor (the ratio of the Freedericksz thresholds in the transparent and dye-doped NLCs) was $\eta = 40$ ($\lambda = 488\,\text{nm}$). The ratio $\eta_\alpha = \eta/(\alpha_{||} + 2\alpha_\perp)$, independent of dye concentration, proved to be $\eta_\alpha = 0.1\,\text{cm}$.

The aberration pattern developed in $\sim 10\,\text{s}$ after starting illumination is not completely stable. At a long-term ($\sim 1\,\text{h}$) illumination, the pattern is significantly transformed. Thus, at oblique light incidence ($\alpha = 50°$, $\lambda = 473$ or $515\,\text{nm}$) the ring number first decreases to zero in 60 min and then increases again. In this case, the sign of the light self-action changes from the positive (self-focusing) to the negative (self-defocusing).

When the light beam was blocked, after the 30–60-min illumination, for $\leq 1\,\text{min}$ (the time sufficient for the director relaxation), the aberration pattern is observable immediately after resuming illumination. Then, this pattern is restored to its initial shape (before light blocking) during $\sim 1\,\text{min}$. Such behavior implies the occurrence of the memorized director field deformation (photoalignment) [18].

At $\lambda = 473\,\text{nm}$ and $\alpha = 50°$, the ring number of the aberrational self-defocusing due to the director rotation at the surface approached 8. In this case, the director rotation at the NLC substrates becomes noticeable after 25-min exposure to light beam.

At normal light incidence, a decrease in the aberration-pattern size was also observed at the long-term (about 10 min) irradiation;

no self-defocusing was manifested in this case. This suggests the contribution of the dye photodestruction.

Light Interaction with Planarly Aligned NLCs

The light-beam self-action in planar cell is qualitatively different from the phenomena in transparent and dye-doped NLCs where the aberration pattern represents a set of rather symmetric concentric rings. For NLC doped with DEANS, in the spectral range 458–515 nm the intensity profile in the cross-section of the transmitted beam can have a quite different form.

The experimental results obtained for $\lambda = 458$, 473, 488 и 515 nm coincide qualitatively. We shall present detailed description for $\lambda = 473$ nm.

At any angle of the light beam incidence on the NLC cell, a complex aberration pattern was developed. This pattern could represent a system of vertical stripes. The times of its development and relaxation were $\sim$10–50 s. The shape of the pattern depends on the light beam power P and the incidence angle α.

At the normal incidence and low beam power $P < 1$ mW no aberrations were observed. At higher power, the ring-shaped aberration pattern appears immediately ($t < 0.1$ s) after starting NLC irradiation (thermal self-defocusing). Further, this pattern changes its shape during $\sim$10 s. At $P = 1$–2 mW a pronounced "stripe" is seen in the steady-state pattern. As the beam power increased, the stripe transformed into two spots (over the appearing ring structure). When the cell was shifted above (with respect to the beam axis), the upper part of the stripe (or upper spot) turned brighter.

At the oblique incidence of the light beam with the power in the range 1–4 mW, a complex pattern asymmetric with respect to the incident-beam axis appeared. The time of its development was $\sim$5–7 s and the relaxation time was $\sim$7–10 s, which corresponds, e.g., to the director reorientation.

For the beam power $P = 1$ mW, where the thermal contribution is minimum, the aberration pattern at $\alpha = 20^\circ$ represents a bright spot, shifted to the left with respect to the incident-beam axis, and a system of arcs, also displaced to the left. At $\alpha = 50^\circ$, the pattern has much larger size and consists of a system of vertical stripes located, mainly, to the left from the incident-beam axis (Fig. 3a). The outer left stripe has maximum width and height. For the case under consideration (positive α), the asymmetry of the aberration pattern is illustrated by Figure 4. It is worth noting that the stripes in the pattern can be

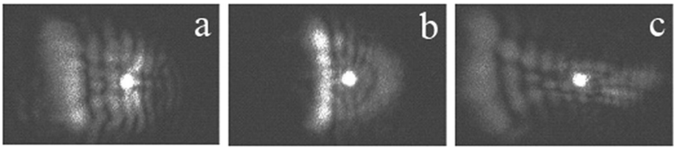

FIGURE 3 Aberrational patterns at oblique ($\alpha = +50°$) incidence of the light beam ($\lambda = 473$ nm, P = 2 mW) on the planar cell ZhKM-1277 + 0.1% DEANS: (a) the steady-state pattern, (b) the pattern upon shifting NLC to the right, (c) the pattern upon shifting NLC to the left. Horizontal angular dimension of each frame is 0.1 rad. Bright spots are due to the ordinary wave produced by a minor rotation of polarization plane with respect to the plane of incidence. The spot location corresponds to the beam position before self-action development.

somewhat bent and the position of the centers of curvature depends on the beam power.

When the NLC cell was shifted relative to the beam axis, the aberration pattern was transformed in a complex way. Thus, for the pattern shown in Figure 3a the upper part turns brighter upon NLC shift upwards. This implies that the refractive index is higher on the beam axis, like the case of the self-focusing [4]. For the horizontal shift, the pattern transformation depends on the displacement direction. Upon shifting the NLC cell to the right (along the **s** vector in Fig. 4), the vertical stripes on the left side of the pattern move to the center and an additional ring-shaped structure appears on the right side (Fig. 3b). Shifting the NLC to the left (opposite to **s**) led to the transformation of the pattern to the shape of a ring sector (Fig. 3c).

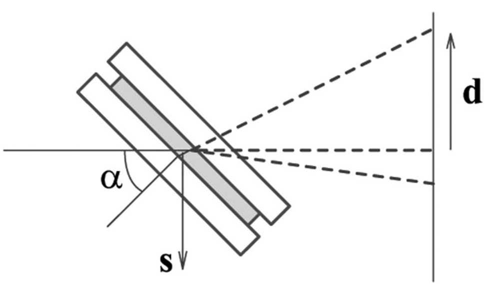

FIGURE 4 Geometry of light interaction with NLC: α is the angle of light incidence and **d** is the direction of the steady-state pattern asymmetry. The vector **s**, characterizing the direction of the NLC shift with respect to the beam axis (see Figs. 3b and 3c), is also shown.

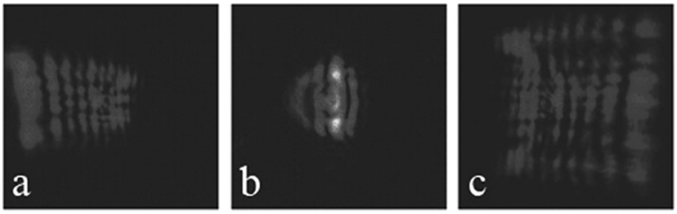

FIGURE 5 Aberration patterns at different angles of incidence of the light beam ($\lambda = 473\,\text{nm}$, $P = 2\,\text{mW}$) on the planar cell ZhKM-1277 + 0.1% DEANS: (a) $\alpha = +50°$, (b) $\alpha = 0°$, and (c) $\alpha = -50°$.

Changing the sign of the angle α alters the asymmetry direction of the pattern (Fig. 5), i.e., the direction of vector **d** in Figure 4.

The pattern asymmetry cannot result from the orientational or thermal light action. It resembles the asymmetry found for NLCs subjected to the combined action of light and DC electric fields [19,20]. In our case, the external DC field affects the pattern shape as well. The asymmetry direction depends on the voltage polarity (Fig. 6). If no voltage is applied, the pattern is elongated to the left with respect to the central spot (Fig. 6a). The positive voltage increases the divergence of the left part of the pattern (Fig. 6b), while the negative one reverses the asymmetry direction (Fig. 6c). Further increase of the negative voltage enlarges the right part.

Low-frequency AC field ($\nu = 3\,\text{kHz}$) suppresses the pattern at oblique incidence of the light beam. At the normal incidence, the voltage leads to increasing, at first, the pattern width and, then, its height.

The rotation of the polarization plane from the horizontal to the vertical (i.e., from the extraordinary to the ordinary wave) decreases the pattern size (Fig. 7). Exactly the same patterns were obtained (during

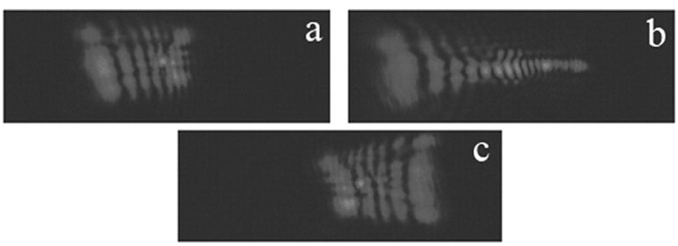

FIGURE 6 Aberration patterns at oblique ($\alpha = +50°$) incidence of the light beam ($\lambda = 473\,\text{nm}$, $P = 2\,\text{mW}$) on the planar cell ZhKM-1277 + 0.1% DEANS under DC voltage: (a) $U = 0$, (b) $U = +1.5$, and (c) $U = -1.5\,\text{V}$.

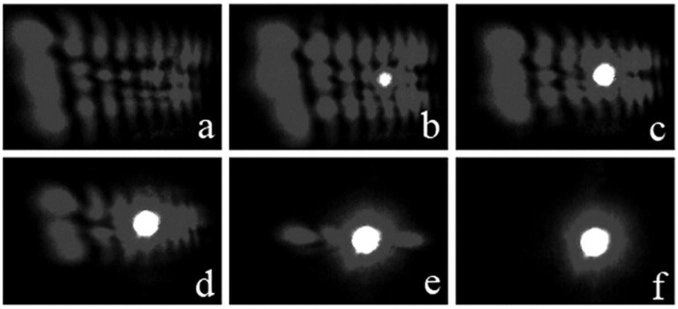

FIGURE 7 Aberration patterns at oblique ($\alpha = +50^\circ$) incidence of the light beam ($\lambda = 473\,\text{nm}$, $P = 2\,\text{mW}$) on the planar cell ZhKM-1277 + 0.1% DEANS at different angles φ of the polarization plane rotation: $\varphi =$ (a) 0°, (b) 10°, (c) 30°, (d) 50°, (e) 70°, (f) 90°. The value $\varphi = 0^\circ$ corresponds to the extraordinary wave; $\varphi = 90^\circ$, to the ordinary one. Other values of φ correspond to the superposition of these waves.

5–7 s) using the beam with initially rotated polarization plane. If the NLC was irradiated by the ordinary wave for $\sim 10\,\text{s}$, the striped structure appears without delay at rotating the polarization plane (adding the extraordinary wave component).

The polarization dependence observed suggests that inhomogeneous distribution of the extraordinary-wave refractive index, leading to the striped diffraction pattern, is formed already under the ordinary-wave action. The rotation of the polarization visualizes and enlarges the pattern.

As mentioned above, the results for different wavelengths in the spectral range 458–515 nm are qualitatively the same. However, there are minor differences. Thus, in the case of normal incidence of the light beam with $\lambda = 458\,\text{nm}$, we observed thermal rings, which transformed into stripes with time. For $\lambda = 515\,\text{nm}$, no striped structure developed at normal light incidence. At $\lambda = 532\,\text{nm}$, the aberration pattern could represent a system of highly distorted asymmetric rings.

For the ZhKM-1277 cell with lower DEANS concentration (0.025 wt %), the pattern at large ($\alpha \geq 60^\circ$) angles of light incidence was ring-shaped. As the incidence angle decreased, a vertical stripe showed up in the pattern center.

For the liquid-crystalline material ZhKM-13N doped with DEANS (0.1 wt %), the aberration pattern at 458 nm ($\alpha = 50^\circ$, $P = 2\,\text{mW}$) had the form of the self-focusing ring, highly elongated in the vertical direction. An increase in the beam power up to 5 mW transformed the ring into a vertical stripe. Application of the AC voltage

(3 V) suppressed the pattern. For the beam with $\lambda = 473\,\text{nm}$, the competition between the thermal (self-defocusing) and orientational (self-focusing) effects took place. No anisotropy of the aberration pattern was observed in this case.

DISCUSSION

The qualitative deviation of the aberrational patterns for planar DEANS-doped NLCs from the conventional ring-shaped pattern suggests that the mechanism involved in the pattern formation is nor heating, neither director reorientation due to light action on the induced dipoles or due to the change in the intermolecular forces at light absorption. This mechanism should, obviously, be characterized by a particularly strong nonlocality of the nonlinear optical response.

The insufficiency of the above phenomena for the explanation of the light self-action in DEANS-doped nematic is also confirmed by the following experimental results. At $P = 1\,\text{mW}$ and the normal light incidence on the planar NLC, the transmitted-beam divergence is rather low. Because the thermal nonlinearity in this geometry is maximum, we can conclude that heating plays no important role in the aberration pattern formation at this beam power. The angle of the "Conventional" light-induced director rotation (and the corresponding change in the refractive index) strongly depends on the light polarization; for the ordinary wave incident on the planar NLC no rotation should occur at all. In our experiment however the director rotation under the ordinary wave does take place.

The observed pattern behavior can be due to the photorefractive effect, i.e., the director rotation under electric field produced by photoinduced charges. The photorefractive effect can be of the bulk [21,22] or surface [23,24,19,20] origin. In the former case, the efficiency of the charge generation in the NLC bulk should depend on absorption and, hence, on the light beam polarization. Subsequent spatial separation of the charges of different sign (due to their different mobilities) produces the electric field responsible for the director reorientation. In the latter case, light affects the concentration of the charges situated near the NLC surface. The efficiency of the surface photorefractivity is independent of the light polarization [19,20].

In our experiment, the aberration pattern changes its size and shape upon the polarization plane rotation. Therefore, we assume that the bulk photorefractivity plays a key role in the formation of the observed pattern.

Let us consider the formation of the aberration pattern owing to the bulk photorefractive effect. The efficiency of the charge generation is, obviously, proportional to the light intensity. In our case, the charges are produced most effectively near the input substrate due to strong decay of the light wave. Let us assume that the mobility of the positive charges is higher than that of the negative ones. Then, the charge distribution can be thought of as shown in Figure 8.

The electric field created by the spatially separated charges results in an asymmetric (relative to the beam axis) director rotation and the respective change in the refractive index profile. To the left of the beam axis, the director will mainly rotate to the direction of the light field **E**, which will increase the refractive index of the extraordinary wave (Fig. 9).

According to this scheme, the most intense central ray of the incident beam (point 1) will be deflected to the left (which agrees with the experiment, Fig. 3a). When the beam axis is shifted to point 2 (the NLC cell is shifted to the right), the central ray is less deflected (Fig. 3b), until the director field reorientation in compliance with the new beam position. When NLC cell is shifted in the opposite direction, the horizontal divergence is maximal (Fig. 3c).

The transformation of the aberration pattern under external DC electric field (Fig. 6) also can be explained by the bulk photorefractivity. Indeed, application of the voltage should move the region of the less mobile charges to the input or output NLC cell substrate, depending on the voltage polarity. In the first case, this would increase the horizontal gradient of the refractive index and elongate the aberration

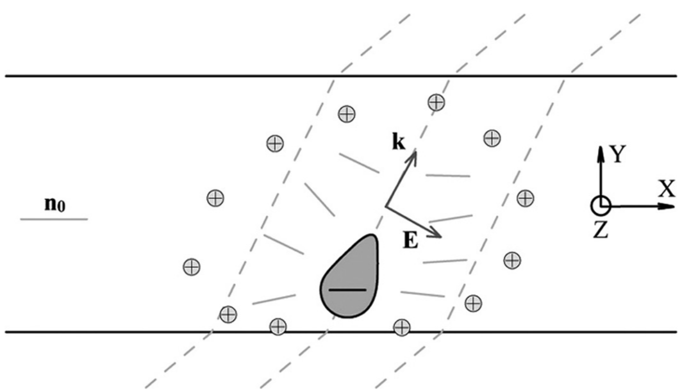

FIGURE 8 The photoinduced-charge distribution and the corresponding director field in the case of the planar NLC illumination by a light beam. **E** and **k** are the electric field and the wave vector of light.

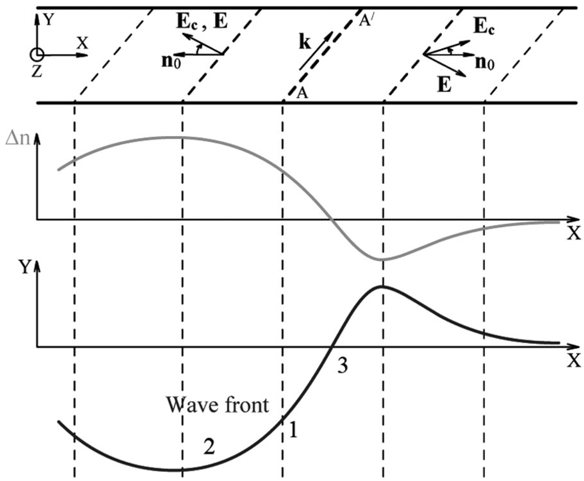

FIGURE 9 The transformation of the refractive-index and the wavefront profiles in the horizontal cross section of the NLC cell: (1) initial position of the beam axis, (2) the position of the "probe-beam" axis after shifting the cell to the right, and (3) the position of the "probe-beam" axis after shifting the cell to the left.

pattern. In the second case, the aberration pattern would gradually transform into its mirror image with respect to the vertical. Our experimental data agree with this scheme: the pattern nothing but increases for one (positive) polarity and changes the degree and direction of asymmetry for another (negative) polarity. At $U = -1.5\,V$, the pattern is the mirror image of the initial one. Such a behavior agrees with our assumption on the lesser mobility of the negative charges. The detailed description of the light beam interaction with photorefracrive dye requires the solution of the self-consistent problem of charge generation and motion, light wave decay, and director reorientation.

CONCLUSION

Light beam interaction with nematic liquid crystals doped with stilbene dye has been studied experimentally.

The light self-action in homeotropic cell is of orientational origin and exhibits main features of the Freedericksz transition. The dye-induced nonlinearity is about 40 times higher than that of the undoped nematic host. Under rather long illumination (tens of minutes) the memory effect occurred.

For the planar sample, we observed for the first time an aberration pattern with a complex asymmetric distribution of the intensity, qualitatively different from the conventional system of the concentric rings. At low power (≤ 2 mW) of obliquely incident beam the pattern represented a system of vertical stripes. The shape and size of the aberration pattern depended on the light beam polarization; the director field deformation occurred even in the case of the ordinary wave. The study of the phenomenon allowed us to assume that this pattern is due to the bulk photorefractive effect.

REFERENCES

[1] Janossy, I., Csillag, L., & Lloyd, A. D. (1991). *Phys. Rev. A*, *44*, 8410.
[2] Barnik, M. I., Zolot'ko, A. S., Rumyantsev, V. G., & Terskov, D. B. (1995). *Crystallogr. Rep.*, *40*, 691.
[3] Janossy, I. & Szabados, L. (1999). *Phys. Rev. E*, *58*, 4598.
[4] Kitaeva, V. F., Zolot'ko, A. S., & Barnik, M. I. (2000). *Mol. Materials*, *12*, 271.
[5] Janossy, I. (1994). *Phys. Rev. E*, *49*, 2957.
[6] Marrucci, L. & Paparo, D. (1997). *Phys. Rev. E*, *56*, 1765.
[7] Zolot'ko, A. S. (1998). *JETP Lett.*, *68*, 437.
[8] Sun, S. T., Gibbons, W. M., & Shannon, P. J. (1992). *Liq. Cryst.*, *12*, 869.
[9] Terskov, D. B., Zolot'ko, A. S., Barnik, M. I., & Rumyantsev, V. G. (1996). *Mol. Materials*, *6*, 151.
[10] Khoo, I. C., Shih, M. Y., Wood, M. V., & Chen, P. H. (2000). *Synth. Met.*, *115*, 145.
[11] Khoo, I. C., Wood, M. V., Shih, M. Y., & Chen, P. H. (1999). *Opt. Exp.*, *4*, 432.
[12] Barnik, M. I., Kharchenko, S. A., Kitaeva, V. F., & Zolot'ko, A. S. (2002). *Mol. Cryst. Liq. Cryst.*, *375*, 363.
[13] Kharchenko, S. A. (1998). Bachelor Thesis, Moscow Institute of Physics and Technology.
[14] Budagovsky, I. A., Ochkin, V. N., Smayev, M. P., Zolot'ko, A. S., & Barnik, M. I. (2007). *Proc. SPIE*, *6729*, 67293E.
[15] Zolot'ko, A. S., Kitaeva, V. F., & Terskov, D. B. (1994). *JETP*, *79*, 931.
[16] Zolot'ko, A. S., Kitaeva, V. F., Kroo, N., Sobolev, N. N., Sukhorukov, A. P., Troshkin, V. A., & Chillag, L. (1984). *JETP*, *60*, 488.
[17] Zolot'ko, A. S., Kitaeva, V. F., Sobolev, N. N., Fedorovich, V. Yu., Sukhorukov, A. P., Kroo, N., & Csillag, L. (1993). *Liq. Cryst.*, *15*, 787.
[18] Barnik, M. I., Kitaeva, V. F., & Zolot'ko, A. S. (2003). *Mol. Cryst. Liq. Cryst.*, *391*, 111.
[19] Budagovsky, I. A., Zolot'ko, A. S., Kitaeva, V. F., Ochkin, V. N., Smayev, M. P., & Barnik, M. I. (2006). *Bulletin of the Lebedev Physics Institute*, no. *3*, 18.
[20] Zolot'ko, A. S., Budagovsky, I. A., Kitaeva, V. F., Ochkin, V. N., Shakun, A. V., Smayev, M. P., & Barnik, M. I. (2006). *Mol. Cryst. Liq. Cryst.*, *454*, 415.
[21] Rudenko, E. V. & Sukhov, A. V. (1994). *JETP*, *78*, 875.
[22] Wiederrecht, G. P., Yoon, B. A., & Wasielewski, M. R. (1995). *Science*, *270*, 1794.
[23] Pagliusi, P. & Cipparrone, G. (2002). *Appl. Phys. Lett.*, *80*, 168.
[24] Boichuk, V., Kucheev, S., Parka, J., Reshetnyak, V., Reznikov, Yu., Shiyanovskaya, I., Singer, K. D., & Slussarenko, S. (2001). *J. Appl. Phys.*, *90*, 5963.